Micromonas polaris, the dominant picophytoplankton species in the Arctic, is probably not a mixotroph

Valeria Jimenez[1], **Florence Le Gall**[1], **John A. Burns**[3], **and Daniel Vaulot**[1, 2 *]

[1]Sorbonne Université, CNRS, UMR7144, Ecology of Marine Plankton team, Station Biologique de Roscoff, 29680 Roscoff, France

[2]Asian School of the Environment, Nanyang Technological University, 50 Nanyang Avenue, Singapore 639798

[3]Sackler Institute for Comparative Genomics and Division of Invertebrate Zoology, American Museum of Natural History, New York, NY, USA

[*]Corresponding author: vaulot@gmail.com

ABSTRACT

Write here abstract

Submitted to: The ISME Journal

Date: September 20, 2019

Introduction

The Arctic is currently undergoing massive changes due to global warming and climate change. These changes are affecting the Arctic ecosystem at higher rates than anywhere else[1–3], with strong and unprecedented effects for Arctic marine ecosystems where phytoplankton production plays an essential role in food webs dynamics and biogeochemical cycles[4–6]. Considerable and variable spatial and temporal changes in Arctic primary production have been observed in the last two decades[5,7,8]. Rapid melting and early ice retreat is increasing the open areas expose to solar radiation showing a considerable increase in spring, summer and annual net primary production as well as a lengthening of the phytoplankton growing season[5,6,8]. Overall changes in Arctic primary production are also influenced by the increase of freshwater delivery to the upper ocean that leads to stronger water column stratification limiting the flux of nutrients to the surface[6,9–14].

Our ability to explain and predict the responses of Arctic phytoplankton communities to climate change are challenged by the limited understanding regarding their ecological and physiological strategies to grow and survive under the present extreme polar environmental conditions such as nutrient limitation and the strong year round seasonal changes in light levels caused by the extent of snow coverage and ice thickness, and the exposure to a long period of darkness (polar winter) (Berge etal 2015). In this extreme and variable context, it has been suggested that mixotrophy (ability to combine photosynthesis and bacteria phagocytosis; bacterivory) could be a common trophic strategy among Arctic protists (Stoecker and Lavrentyev 2018). Worldwide, mixotrophy is an important, but until recently underestimated, process for energy and nutrient transfer (e.g. carbon fluxes) through out the food web[15–23]. Mixotrophic plankton are widespread in the ocean and can be found everywhere across the tree of life[24] and can account for a large part of bacterivory in aquatic environments[18,19,25]. Moreover, model predictions suggest that when mixotrophs are taken into account in trophic network analysis, the transfer of biomass to higher trophic levels increases and higher mean organism size and sinking carbon fluxes are predicted[26]. In the warming Arctic, mixotrophs could outcompete diatoms?? outcompete

specialists

The ongoing increase in stratification and nutrient limitation in the Arctic have been associated with the observed increase of the smaller phytoplankton (picophytoplankton: 2-3 μm cell diameter)[27,28] composed by cold-adapted eukaryotes since cyanobacteria are nearly absent in polar marine ecosystems[29]). Among the picophytoplankton community, the green algae *M. polaris*,[30,31] currently dominates in the Arctic ocean[30,32–35] and its abundance is expected to increase as the Arctic ocean warms and the stratified oligotrophic areas expand[27,36]. *M. polaris* physiological plasticity that allows it to currently dominate the Arctic picoeukaryote community as well as thrive under the climate driven changes observed in the Arctic, is not yet well understood. *M. polaris* was shown in the laboratory, to positively respond to the combination of warming and acidification by increasing growth rates and biomass production[36]. Mixotrophy may be another advantageous trait that contributes to the success of *M. polaris* in the Arctic. *Micromonas* has been described as a mixotroph in laboratory and field experiments[37–40]. More than 25 years ago, Gonzales et al.[40] reported mixotrophy in a temperate *Micromonas* strain (*M. pusilla*) based on a positive acid lysozyme assay and ingestion of fluorescenty labelled bacteria (FLBs). More recently, *Micromonas*, has been hypothesized to be able to consume bacterioplankton using FLBs and yellow-green fluorescent microspheres as preys in in-situ experiments with pico and nanoplankton microbial communities. A *Micromonas*-like picoeukaryote (based on its shape and analysis of denaturing gradient gel electrophoresis (DGGE) band sequencess) was reported to ingest a significant amount of the preys offered[39]. The ingestion of beads was then tested in *M. polaris* strain CCMP2099 under laboratory conditions that compared different light levels (50 μE m^{-2} s^{-1} and dark) and nutrient concentrations (full strength and 10-fold diluted media). The highest grazing rates were observed under light and low nutrient conditions[37,38]. ADD Micromonas RNAseq paper[38]

In the present paper, we analyse mixotrophy in a number of *M. polaris* strains, (including the strain tested by McKie-Krisberg et al.[37]) isolated from different regions and depth in the Arctic Ocean, using FLBs and YG-beads as prey and flow cytometry, which allows to quantify a large number of cells compared to epifluorescence microscopy used in previous studies[37,39,40]). De-

spite extensive experimental work, we found no evidences of mixotrophy. In addition, predictions from *in silico* gene-based phagocytocis model[41] based on the available genomes (ref; Worden) and transcriptomes (ref; MMETSP, other?) of the genus *Micromonas*, do not reveal any sign of potential phagocytocis.

********** OTHER TEXT: NEED TO ADD EXAMPLES OF MIXOTROPHY The degree of combination of the two trophic modes (phototrophy and phagotrophy) in each mixotrophic speacies is affected primarily by light, nutrient concentrations, and prey availability and quality (refs). A number of mixotrophic species are primarily phototrophs and feed under light limitation or when essential nutrients are scarce. Maintaining this trophic plasticity is energetically costly - shifts between bacterivory and photosynthesis.

Under prolonged periods of darkness or low irradiance, mixotrophs could still survive despite the lack or reduce rates of photosynthesis. by supplementing their carbon requirements that are limited by the lack or reduce rates of photosynthesis (Millette etal 2017, Zhang etal 1998, Stoecker and Lavrentyev 2018, Stoecker etal 2016), and under oligotrophic conditions mixotrophy can supply the cell with the limiting nutrients (Stoecker etal 2016).

Phytoplankton species-specific strategies to survive in this variable and extreme environment determines important ecological processes including the succession of phytoplankton blooms in the winter to spring transition (refs).

Materials and Methods

Strains and culturing condition

Bacterivory was studied in four *M. polaris* strains and one mixotrophic *Ochromonas triangulata* strain that was used as a positive control. Three of the *M. polaris* strains (RCC2306, RCC4298 and RCC2258) and *O. triangulata* strain RCC21, were obtained from the Roscoff Culture Collection (http://www.roscoff-culture-collection.org/) and the fourth *M. polaris* strain (CCMP2099) was obtained from the Provasoli-Guillard National Center for Culture of Marine Phytoplankton and Microbiota (https://ncma.bigelow.org). *M. polaris* strains were isolated from different locations and depth in the Arctic (Table 1). All strains were non-axenic and grown under a 12h:12h

light:dark cycle at 80 μE m^{-2} s^{-1} PAR using L1 medium[42] made with artificial sea water (ASW)[43]. All *M. polaris* strains were grown at 4 °C and *O. triangulata* at 20 °C. Cells were acclimated and maintained in mid-exponential growth phase before the beginning of each experiment.

Experimental design

To test feeding, three different experimental designs were performed with *M. polaris* strains and another four with *O. triangulata*. Feeding was primarily tested using yellow-green fluorescent polystyrene-based microspheres (YG-beads; 0.5 μm in diameter, Fluoresbrite, Polysciences, Inc., Warrington, PA, USA) as preys, and in some cases fluorescently labelled bacteria (FLBs) were used. FLBs were prepared according to the protocol of[44] using the bacteria *Brevundimonas diminuta* (strain CECT313, also named *Pseudomonas diminuta*), obtained from the Spanish Type Culture Collection (CECT, Valencia, Spain).

In experiment type 1 (*M. polaris*-EXP1) feeding was tested for each *M. polaris* strain grown under four different culture conditions. Each treatment was carried out (in duplicates for RCC2306 and RCC4298 and triplicates for RCC2258 and CCMP2099) by transferring a small volume of culture, previously maintained in mid-exponential growth, to L1-ASW medium (replete) or ASW (starved) and then placed in the dark or left in the same light conditions as for culture maintenance. Each treatment (Light-replete, Light-starved, Dark-starved and Dark-replete) was followed up for 15-17 days and feeding was tested with YG-beads on day 7 (Feeding 1) and after 14-17 days of incubation (Feeding 2).

Experiment type 2 (*M. polaris*-EXP2) was performed with *M. polaris* strain RCC2306 and RCC2258 and was set-up the same way as EXP1 (in triplicates), but with an additional treatment (Light-replete-Ab) were 1 μl of PBS antibiotics (Sigma Aldrich P4083) per 1 ml of culture were added at the beginning of the experiment. Moreover, the five treatments were incubated for only one week and feeding was tested with YG-beads at the end of the incubation (Day 7).

To compare feeding on YG-beads and FLBs, a third type of experiment (*M. polaris*-EXP3) was performed with *M. polaris* RCC4298. For each prey type (YG-beads and FLBs) feeding was tested in triplicate in mid-exponential phase cultures (Light-replete) (Table 2).

For all experiments (*M. polaris*-EXP1 to EXP3), the initial concentration for each treatment was 5 x 10^5 cells ml^{-1}.

The experimental design of two of the experiments performed with *O. triangulata* was the same and only differed in their replication and number of feeding time points. *O. triangulata*-EXP1 was conducted in duplicates and with three feeding time points (T0, T20 and T40 minutes), and *O. triangulata*-EXP2 in triplicates and two feeding time points (T0 and T40 minutes). Feeding was tested under two different culture conditions by transferring a small volume of culture, previously maintained in mid-exponential growth, to L1-ASW medium (Light-replete) or ASW (Light-starved) and incubated in the same light conditions as for culture maintenance. After one week of incubation, feeding was tested with YG-beads (Table S1). The third experiment type (*O. triangulata*-EXP3) was performed in parallel with *M. polaris*-EXP3 to compare feeding on YG-beads and FLBs. For each prey type (YG-beads and FLBs) feeding was tested in biological triplicates in mid-exponential phase cultures (Light-replete) (Table 2). In a fourth experiment type (*O. triangulata*-EXP4a and b) feeding was tested using FLBs as prey in Light-replete culture conditions. This experiment type was performed two times (a and b) and each time in duplicates (Table S1 and Supplementary Data S1).

The degree of attachment of YG-Beads to cells, immediately after the addition of prey (T0 minutes), was also quantify in a number of additional experiments (*M. polaris*-AdEXP) performed with *M. polaris* strains RCC2306 and RCC4298. For *M. polaris* strain RCC2306 the quantification was done in cultures grown under Light-replete, Light-starved and Dark-replete conditions, and for *M. polaris* strain RCC4298 with cultures grown under Light-replete-Ab, Light-replete, Light-starved, Dark-starved and Dark-replete conditions (Supplementary Data S1).

Cell monitoring, feeding estimates and sample fixation

Cultures in mid-exponential growth and under the different experimental conditions were monitored live, using a Guava easyCyte (Luminex Corporation, USA) flow cytometer (FCM), to determine cell counts and cellular parameters based on forward angle light scatter (FALS – a proxy of cell size) and red autofluorescence from chlorophyll (X $\pm$ X nm band pass filter) with

data collection triggered on FALS (excitation laser of 488 nm). Flow cytometry was also used to determine the percent of cells with preys (YG-beads and FLBs) in fixed samples (modification from protocol in[45], with data collection triggered on FALS and green fluorescence (525 $\pm$ 30 nm band pass filter). When triggering on FALS, cells that contained red autofluorescence from chlorophyll as well as green fluorescence (same signal as the prey added; YG-beads or FLBs) were considered to be cells containing prey (Fig. S1). In addition, to confirm the total concentration of prey added to each flask, the sample was also run triggered on green fluorescence. FCM listmodes were analyzed with the Guava easyCyte Suite Software 3.1 (Luminex Corporation, USA). For each feeding experiment, the ingestion of prey was quantified in each experimental flask by the addition of prey (1.5 to 2.5 prey per cell) and the subsequent sub-sampling and fixation after 0, 20 and 40 minutes of incubation with prey. The 0 minutes (T0) sample accounts for the coincidental attachment of prey to the cell, therefore the percent of cells ingesting prey corresponds to the percent of cells with prey at time points T20 or T40, minus the percent of cells with prey at T0.

Cell fixation at each feeding time point was performed with acid Lugol's iodine solution and formaldehyde 3.7%, and cleared with sodium thiosulfate 3% following the protocol in[45].

Prediction model analysis

JB

Statistical analyses

Statistical analysis were performed in R[46], using a t-test or linear mixed model analysis.

********** MAYBE Add??? Other experiments; lysosensor, different beads sizes, continuous live run for 20 minutes.

Results

Changes in growth and cellular parameters

A slight modification of the protocol described in[45] was used to determine the percent of cells feeding on YG-Beads or FLBs. To quantify the percent of cells with prey we used flow cytometry which allowed us to screen a large number of cells per sample (xxx) compared to the use of filtration and epifluorescence microscope that typically comprises the examination of 100 to 200 cells per sample. To validate the use of flow cytometry we used a positive control (The mixotroph; *O. triangulata* strain RCC21). In the four experiments performed with *O. triangulata* (*O. triangulata*-EXP1 to EXP4) we observed feeding on YG-Beads and FLBs that ranged from 6 to 14 and 20 to 27 percent of cells feeding on each prey type respectively (Table 2 and S1). In contrast to the results obtained for the positive control *O. triangulata*, we did not observed *M. polaris* feeding on either prey type under any of the culture conditions tested.

Primarily, for *M. polaris* feeding was measured in four strains (CCMP2099, RCC2306, RCC4298 and RCC2258) (Table 1) grown under 4 culture conditions (*M. polaris*-EXP1; light-replete, light-starved, dark-replete and dark-starved) incubated over a period of 15 to 17 days, where feeding was examined with YG-beads on day 7 (Feeding 1) and after 14-17 days of incubation (Feeding 2). Clear effects of continuous darkness and nutrient limitation were observed for all strains. Overall, for all 4 strains under dark conditions, growth ceased between day 4 and day 7 and thereafter cell concentration remained stable (same as at the beginning of the experiment) through out the entire incubation (Fig. 1). For cultures grown under low nutrient conditions, a decrease in growth rate was observed after one week of incubation (Fig. 1). Additional signs of the effects of darkness and nutrient starvation were observed in FALS (proxy of cell size) and red chlorophyll fluorescence (Fig. S2). When compared to Light-replete culture conditions, cells incubated in the dark showed a significant decrease in FALS, whereas the effects of nutrient starvation were more variable and strain-specific. For RCC2258 and RCC4298 under starvation, FALS did not change and in the case of CCMP2099 and RCC2306, FALS increased and decreased respectively (Fig. 1 and S2). Changes in red chlorophyll fluorescence

were more variable. For two strains (CCMP2099 and RCC2258) in the dark, red fluorescence was lower than replete conditions whereas for the other 2 strains (RCC2306 and RCC4298) no major differences between dark and Light-replete conditions were observed. Under nutrient starvation (Light-starved), for strains RCC2306 and RCC2258, red fluorescence was significantly lower than Light-replete conditions, whereas for CCMP2099 a significant increase was observed after one week of incubation and for RCC4298 no major changes were observed except for a the last four days were cells under starvation showed the lowest red fluorescence compared to all other culture conditions. Under these four culture conditions, feeding on YG-Beads was not detected for any of the four *M. polaris* strains. For each feeding experiment (Feeding 1 and 2), no significant differences were observed between the percent of cells with YG-Beads at T0 and the subsequent time points (T20 and T40) (Fig. 2).

Feeding of YG-Beads was tested again with an additional experiment (*M. polaris*-EXP2) performed with two of the *M. polaris* strains (RCC2258 and RCC2306). In this experiment an additional culture condition was tested (Light-replete-Ab; replete medium + antibiotics) and the feeding experiment was conducted after one week of incubation in each condition. Once more, feeding was not detected under any of the culture conditions (Fig. S3).

Moreover, *M. polaris* phagocytocis was not observed when using either YG-Beads or FLBs as prey (*M. polaris*, EXP-3). This experiment was conducted simultaneously with the positive control *O. triangulata*, which exhibited a 14 percent of cells feeding on YG-Beads and 26.9 percent of cells feeding on FLBs (Table 2).

Feeding on YG-Beads was not detected (no differences between T0 and subsequent feeding time points) in any of the experiments performed with *M. polaris*, yet we observed differences in percent of cells with YG-Beads that appear to be related to differences in cell concentration. The correlation between percent of cells with YG-Beads and cell abundance (at T0) was studied in all the main experiments performed with *M. polaris* strains and *O. triangulata* (*M. polaris* and *O. triangulata*-EXP1 to EXP3) in combination with a number of additional feeding experiments (*M. polaris*-AdEXP) conducted at different *M. polaris* cell concentrations. A logarithmic significant correlation (R^2 equal to 0.79) was observed where the percent of cells with beads appears to

increase with cell concentration reaching a saturation point where very dense cultures can show up to 50 percent of cells with YG-Beads (Fig. 4).

****** Maybe add: if including, results of lysosensor and continuous run. ******

Prediction model analysis

JB: add here results of prediction model

Discussion

Evidence of phagotrophy in green algae Limitation and darkness effects on mixotrophy attachment vs inside the cell proof

Conclusion

Therefore, if *M. polaris* is mixotroph, this may have profound impacts in present and future predictions of Arctic primary production, because of the importance and increasing concentrations of *M. polaris* in the Arctic Ocean

Based on our results, we suggest that careful consideration should be taking when describing *M. polaris* as a mixotroph. Further analyses should be done to prove the actual *Micromonas* ingestion of prey (e.g. transmission electron microscopy) and growth advantages under a mixotrophic nutritional mode.

References

1. Box, J. E. *et al.* Key indicators of Arctic climate change: 1971–2017. *Environ. Res. Lett.* **14**, 45010, DOI: 10.1088/1748-9326/aafc1b (2019).

2. Wassmann, P. Overarching perspectives of contemporary and future ecosystems in the Arctic Ocean. *Prog. Oceanogr.* **139**, 1–12, DOI: https://doi.org/10.1016/j.pocean.2015.08.004 (2015).

3. Graversen, R. G., Mauritsen, T., Tjernström, M., Källén, E. & Svensson, G. Vertical structure of recent Arctic warming. *Nature* **451**, 53 (2008).

4. Arrigo, K. R., van Dijken, G. & Pabi, S. Impact of a shrinking Arctic ice cover on marine primary production. *Geophys. Res. Lett.* **35**, DOI: 10.1029/2008GL035028 (2008).

5. Kahru, M., Lee, Z., Mitchell, B. G. & Nevison, C. D. Effects of sea ice cover on satellite-detected primary production in the Arctic Ocean. *Biol. letters* **12**, 20160223, DOI: 10.1098/rsbl.2016.0223 (2016).

6. Park, J.-Y., Kug, J.-S., Bader, J., Rolph, R. & Kwon, M. Amplified Arctic warming by phytoplankton under greenhouse warming. *Proc. Natl. Acad. Sci.* **112**, 5921 LP – 5926, DOI: 10.1073/pnas.1416884112 (2015).

7. Tedesco, L., Vichi, M. & Scoccimarro, E. Sea-ice algal phenology in a warmer Arctic. *Sci. Adv.* **5**, eaav4830, DOI: 10.1126/sciadv.aav4830 (2019).

8. Renaut, S., Devred, E. & Babin, M. Northward Expansion and Intensification of Phytoplankton Growth During the Early Ice-Free Season in Arctic. *Geophys. Res. Lett.* **45**, 10,510–590,598, DOI: 10.1029/2018GL078995 (2018).

9. Brown, N. J., Nilsson, J. & Pemberton, P. Arctic Ocean Freshwater Dynamics: Transient Response to Increasing River Runoff and Precipitation. *J. Geophys. Res. Ocean.* **0**, DOI: 10.1029/2018JC014923 (2019).

10. Nummelin, A., Ilicak, M., Li, C. & Smedsrud, L. H. Consequences of future increased Arctic runoff on Arctic Ocean stratification, circulation, and sea ice cover. *J. Geophys. Res. Ocean.* **121**, 617–637, DOI: 10.1002/2015JC011156 (2016).

11. Tremblay, J.-É. *et al.* Global and regional drivers of nutrient supply, primary production and CO2 drawdown in the changing Arctic Ocean. *Prog. Oceanogr.* **139**, 171–196, DOI: https://doi.org/10.1016/j.pocean.2015.08.009 (2015).

12. Slagstad, D., Wassmann, P. F. J. & Ellingsen, I. Physical constrains and productivity in the future Arctic Ocean (2015).

13. Timmermans, M.-L. *et al.* Surface freshening in the Arctic Ocean's Eurasian Basin: An apparent consequence of recent change in the wind-driven circulation. *J. Geophys. Res. Ocean.* **116**, DOI: 10.1029/2011JC006975 (2011).

14. Coupel, P. *et al.* The impact of freshening on phytoplankton production in the Pacific Arctic Ocean. *Prog. Oceanogr.* **131**, 113–125, DOI: https://doi.org/10.1016/j.pocean.2014.12.003 (2015).

15. Caron, D. A. Mixotrophy stirs up our understanding of marine food webs. *Proc. Natl. Acad. Sci. United States Am.* **113**, 2806–2808, DOI: 10.1073/pnas.1600718113 (2016).

16. Mitra, A. *et al.* The role of mixotrophic protists in the biological carbon pump. *Biogeosciences* **11**, 995–1005, DOI: 10.5194/bg-11-995-2014 (2014).

17. Mitra, A. *et al.* Defining Planktonic Protist Functional Groups on Mechanisms for Energy and Nutrient Acquisition: Incorporation of Diverse Mixotrophic Strategies. *Protist* **167**, 106–120, DOI: https://doi.org/10.1016/j.protis.2016.01.003 (2016).

18. Hartmann, M. *et al.* Mixotrophic basis of Atlantic oligotrophic ecosystems. *Proc Natl Acad Sci U S A* **109**, 5756–5760, DOI: 10.1073/pnas.1118179109 (2012).

19. Leles, S. G. *et al.* Sampling bias misrepresents the biogeographical significance of constitutive mixotrophs across global oceans. *Glob. Ecol. Biogeogr.* **28**, 418–428, DOI: 10.1111/geb.12853 (2019).

20. Stoecker, D. K., Hansen, P. J., Caron, D. A. & Mitra, A. Mixotrophy in the Marine Plankton. *Annu. Rev. Mar. Sci.* DOI: 10.1146/annurev-marine-010816-060617 (2016).

21. Stoecker, D. K. & Lavrentyev, P. J. Mixotrophic Plankton in the Polar Seas: A Pan-Arctic Review (2018).

22. Ward, B. A. Mixotroph ecology: More than the sum of its parts. *Proc. Natl. Acad. Sci.* **116**, 5846 LP – 5848, DOI: 10.1073/pnas.1902106116 (2019).

23. Edwards, K. F. Mixotrophy in nanoflagellates across environmental gradients in the ocean. *Proc. Natl. Acad. Sci.* **116**, 6211 LP – 6220, DOI: 10.1073/pnas.1814860116 (2019).

288 **24.** Selosse, M.-A., Charpin, M. & Not, F. Mixotrophy everywhere on land and in water: the
289 grand écart hypothesis. *Ecol. Lett.* **20**, 246–263, DOI: 10.1111/ele.12714 (2017).

290 **25.** Unrein, F., Gasol, J. M., Not, F., Forn, I. & Massana, R. Mixotrophic haptophytes are key
291 bacterial grazers in oligotrophic coastal waters. *ISME J* **8**, 164–176, DOI: 10.1038/ismej.2013.
292 132 (2014).

293 **26.** Ward, B. A. & Follows, M. J. Marine mixotrophy increases trophic transfer efficiency, mean
294 organism size, and vertical carbon flux. *Proc. Natl. Acad. Sci.* **113**, 2958 LP – 2963, DOI:
295 10.1073/pnas.1517118113 (2016).

296 **27.** Li, W. K., McLaughlin, F. A., Lovejoy, C. & Carmack, E. C. Smallest algae thrive as the Arctic
297 Ocean freshens. *Science* **326**, 539, DOI: 10.1126/science.1179798 (2009).

298 **28.** Ward, B. A. Temperature-Correlated Changes in Phytoplankton Community Structure Are
299 Restricted to Polar Waters. *PLOS ONE* **10**, e0135581 (2015).

300 **29.** Paulsen, M. L. *et al.* Synechococcus in the Atlantic Gateway to the Arctic Ocean (2016).

301 **30.** Lovejoy, C. *et al.* Distribution, phylogeny, and growth of cold-adapted picoprasinophytes in
302 arctic seas. *J. Phycol.* **43**, 78–89 (2007).

303 **31.** Simon, N. *et al.* Revision of the Genus Micromonas Manton et Parke (Chlorophyta, Mamiel-
304 lophyceae), of the Type Species M. pusilla (Butcher) Manton & Parke and of the Species M.
305 commoda van Baren, Bachy and Worden and Description of Two New Species Based on the
306 Genetic and . *Protist* **168**, 612–635, DOI: https://doi.org/10.1016/j.protis.2017.09.002 (2017).

307 **32.** Kilias, E., Kattner, G., Wolf, C., Frickenhaus, S. & Metfies, K. A molecular survey of
308 protist diversity through the central Arctic Ocean. *Polar Biol.* **37**, 1271–1287, DOI: 10.1007/
309 s00300-014-1519-5 (2014).

310 **33.** Kilias, E. S., Nöthig, E. M., Wolf, C. & Metfies, K. Picoeukaryote plankton composition off
311 West Spitsbergen at the entrance to the Arctic Ocean. *The J. eukaryotic microbiology* **61**,
312 569–579, DOI: 10.1111/jeu.12134 (2014).

34. Marquardt, M., Vader, A., Stübner, E. I., Reigstad, M. & Gabrielsen, T. M. Strong Seasonality of Marine Microbial Eukaryotes in a High-Arctic Fjord (Isfjorden, in West Spitsbergen, Norway). *Appl. environmental microbiology* **82**, 1868–1880, DOI: 10.1128/AEM.03208-15 (2016).

35. Balzano, S., Marie, D., Gourvil, P. & Vaulot, D. Composition of the summer photosynthetic pico and nanoplankton communities in the Beaufort Sea assessed by T-RFLP and sequences of the 18S rRNA gene from flow cytometry sorted samples. *ISME J* **6**, 1480–1498, DOI: 10.1038/ismej.2011.213 (2012).

36. Hoppe, C. J. M., Flintrop, C. M. & Rost, B. The Arctic picoeukaryote Micromonas pusilla benefits synergistically from warming and ocean acidification. *Biogeosciences* **15**, 4353–4365, DOI: 10.5194/bg-15-4353-2018 (2018).

37. McKie-Krisberg, Z. M. & Sanders, R. W. Phagotrophy by the picoeukaryotic green alga *Micromonas*: implications for Arctic Oceans. *The ISME J.* **10**, 1953–1961 (2014).

38. McKie-Krisberg, Z. M., Sanders, R. W. & Gast, R. J. Evaluation of Mixotrophy-Associated Gene Expression in Two Species of Polar Marine Algae. *Front. Mar. Sci.* **5**, 1–12, DOI: 10.3389/fmars.2018.00273 (2018).

39. Sanders, R. & Gast, R. Bacterivory by phototrophic picoplankton and nanoplankton in Arctic waters. *FEMS microbiology ecology* **82**, 242–253, DOI: 10.1111/j.1574-6941.2011.01253.x (2012).

40. González, J. M., Sherr, B. & Sherr, E. B. Digestive enzyme activity as a quantitative measure of protistan grazing: the acid lysozyme assay for bacterivory. *Mar. Ecol. Prog. Ser.* **100**, 197–206, DOI: 10.3354/meps100197 (1993).

41. Burns, J. A., Pittis, A. A. & Kim, E. Gene-based predictive models of trophic modes suggest Asgard archaea are not phagocytotic. *Nat. Ecol. Evol.* **2**, 697–704, DOI: 10.1038/s41559-018-0477-7 (2018).

338 **42.** Guillard, R. R. L. & Hargraves, P. E. Stichochrysis immobilis is a diatom, not a chrysophyte.
339 *PHYCOLOGIA* **32**, 234–236, DOI: doi:10.2216/i0031-8884-32-3-234.1 (1993).

340 **43.** Keller, M. D., Selvin, R. C., Claus, W. & Guillard, R. R. L. Media for the culture of oceanic
341 ultraphytoplankton. *J. Phycol.* **23**, 633–638 (1987).

342 **44.** Sherr, B. F., Sherr, E. B. & Fallon, R. D. Use of monodispersed, fluorescently labeled bacteria
343 to estimate in situ protozoan bacterivory. *Appl Environ Microbiol* (1987).

344 **45.** Sherr, E. & Sherr, B. Protistan grazing rates via uptake of fluorescently labeled prey. In
345 Kemp, P., Sherr, B., Sherr, E. & Cole, J. (eds.) *Handbook ofMethods in Aquatic Microbial*
346 *Ecology*, 695–701 (Lewis Publishers: Boca Raton, USA, 1993).

347 **46.** R Core Team. *R: A Language and Environment for Statistical Computing*. R Foundation for
348 Statistical Computing, Vienna, Austria (2014).

349 Acknowledgments

350 This study was supported by ANR contract PhytoPol (xxx).

351 Author contributions statement

352 DV and VJ conceived the study. VJ and FLG collected and processed the samples. VJ, JB and
353 DV analyzed the data. VJ and DV drafted the manuscript. VJ, DV and JB edited the final version
354 of the paper.

355 Additional information

356 *Data availability*

357 Processed data and scripts are available from https://github.com/xx.

358 *Competing interests*

359 The authors declare no competing interests.

Table 1. List of *Micromonas polaris* and *Ochromonas triangulata* strains used in this study with isolation Arctic region, depth (m) and culturing growth temperature (°C).

Species	Strain	Origin	Lat Long	Depth	Temp
M. polaris	RCC2306	Arctic, Beaufort Sea	71°N 132°W	70	4
	RCC4298	Arctic, Greenland Sea	82°N 20°E	20	4
	RCC2288	Arctic, Beaufort Sea	70°N 135°W	0	4
	CCMP2099	Arctic, Baffin Bay	76°N 75°W	55	4
O. triangulata	RCC21	Atlantic, Bay of Biscay	48N 4W	-	20

Table 2. Comparison between preys (YG-beads and FLBs) in feeding experiments performed with *Micromonas* and *Ochromonas*. The percent of cells with preys (Mean±sd) is indicated for each time point after the addition of prey (T0 and T40 minutes). The percent of cells feeding on each type of prey corresponds to the difference between T0 and T40.

				Percent of cells with preys		
Species	Strain	Experiment	Prey	T0	T40	Dif T40-T0
M. polaris	RCC4298	*M. polaris*-EXP3	FLBs	24.6±2.3	24.6±2.7	0.0
			Beads	35.6±2.2	34.9±2.0	-0.7
O. triangulata	RCC21	*O. triangulata*-EXP3	FLBs	11.4±2.1	38.3±8.3	26.9
			Beads	17.2±3.0	31.2±6.7	14.0

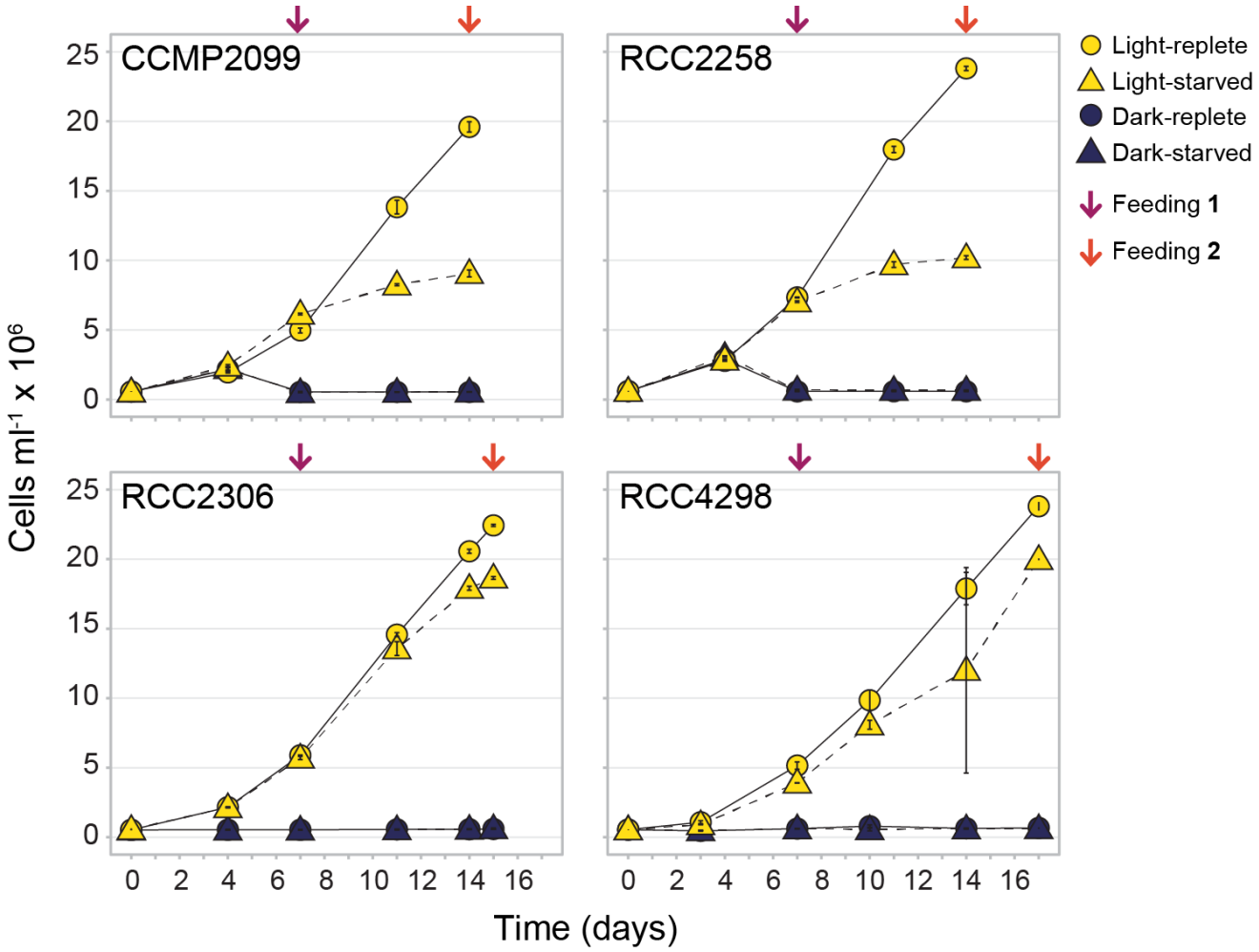

Figure 1. Growth curves for each *M. polaris* strain grown under four treatments (*M. polaris*-EXP1). Arrows indicate the time point (days) when a feeding experiment was performed.

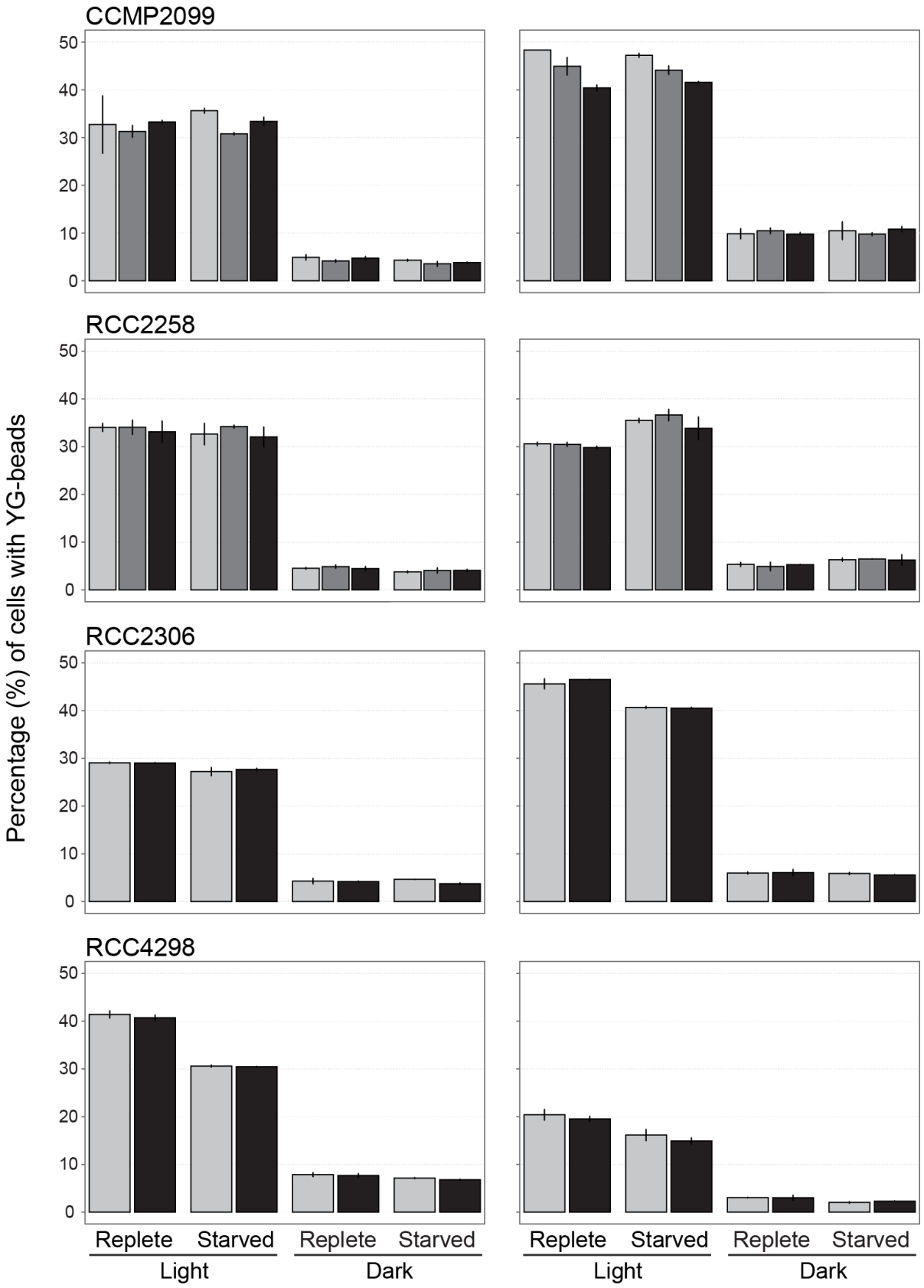

Figure 2. Percent of *M. polaris* cells with YG-beads (*M. polaris*-EXP1) for each strain and treatment at each feeding experiment. The first column correspond to feeding-1 and second column to feeding-2. The color of the bars represent the time point (in minutes) after the addition of YG-beads (0 minutes; light grey, 20 minutes; dark grey, 40 minutes; black).

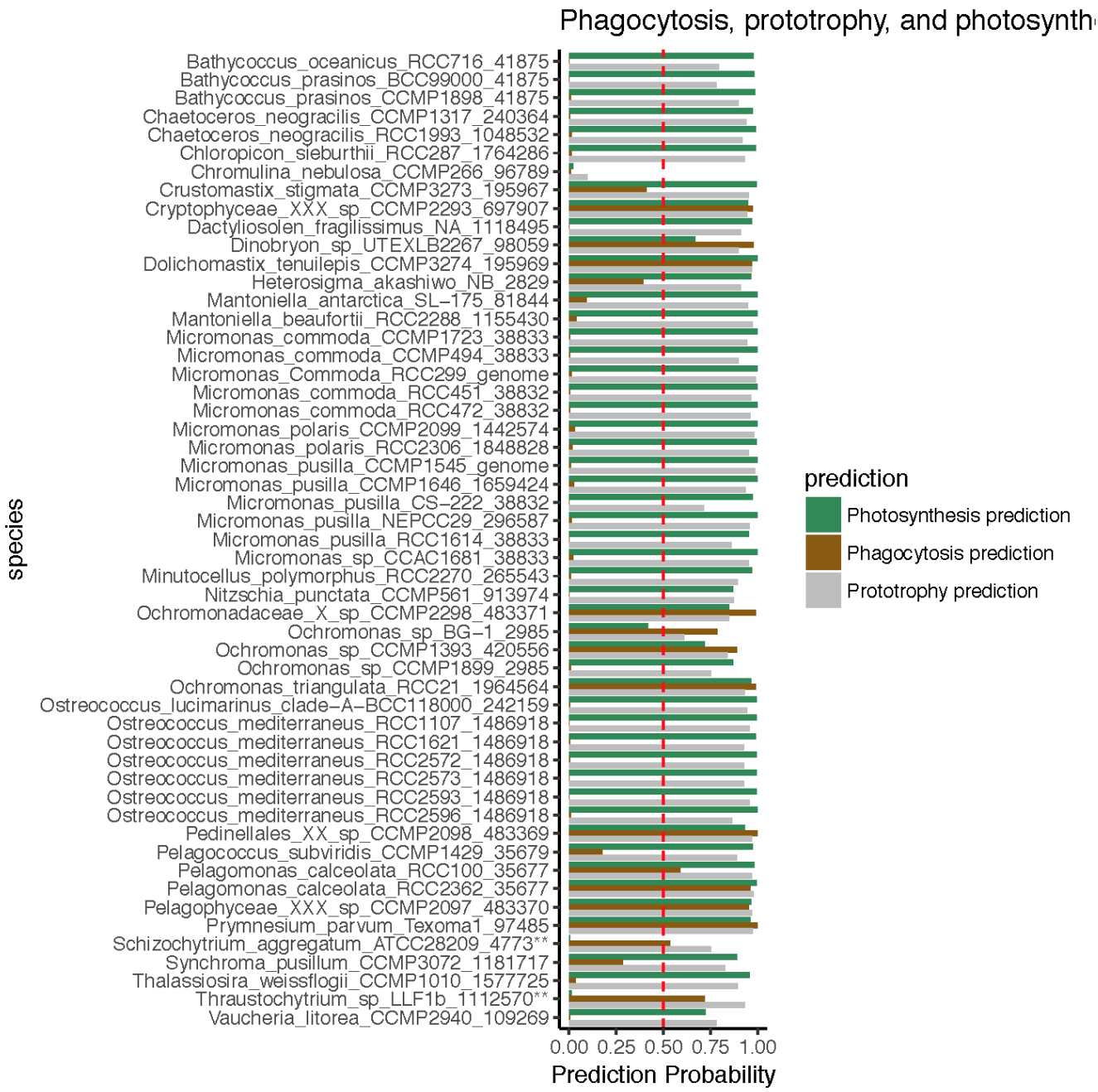

Figure 3. Transcriptome analyses JB.

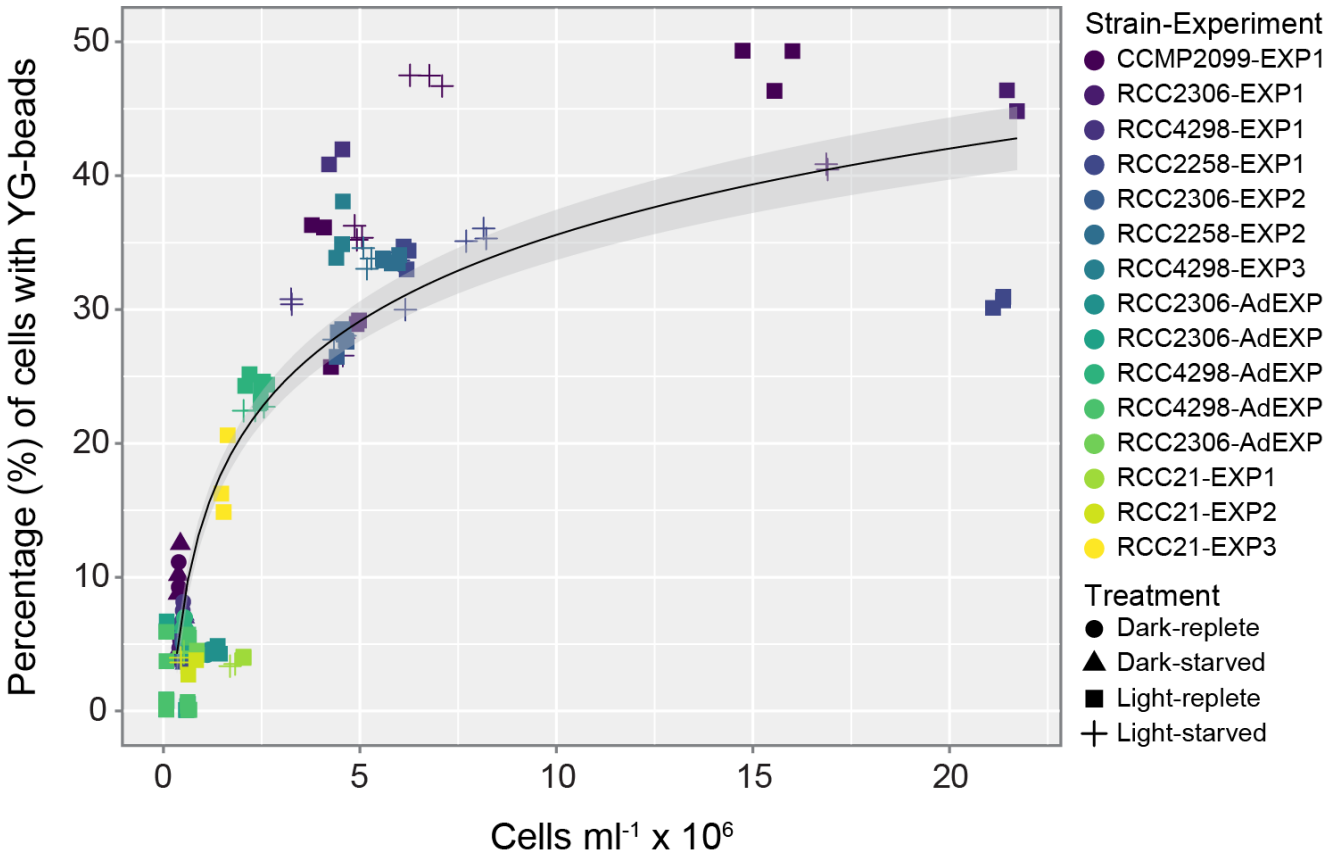

Figure 4. Relationship between percent of cells with YG-beads and cell concentration. The line and spread represents a logarithmic correlation fit with an R^2 equal to 0.79. For each experiment only the time point immediately after the addition of YG-beads (T0 minutes) was considered. *M. polaris* and *O. triangulata* experiments type 1 to 3 were evaluated together with additional experiments with *M. polaris* strains RCC2306 and RCC4298 (Supplementary Data S1).

1 Supplementary material

All supplementary material is available at https://github.com/xx

1.1 Supplementary Data

Supplementary Data S1: Excel sheet with all the data.

Table S1. Additional experiments performed with the positive control *O. triangulata* strain RCC21. The percent of cells with preys (Mean±sd) is indicated for each time point after the addition of prey (T0, T20 and T40 minutes). The percent of cells feeding on each type of prey corresponds to the difference between T0 and T40.

			Percent of cells with preys			
Experiment	Condition	Prey	T0	T20	T40	Dif T40-T0
O. triangulata-EXP1	Light-replete	Beads	4.0±0.1	9.3±0.3	12.3±0.3	8.3
O. triangulata-EXP1	Light-starved	Beads	3.4±0.1	7.6±0.0	9.9±0.4	6.5
O. triangulata-EXP2	Light-replete	Beads	3.3±0.8	n.d.	9.4±2.2	6.2
O. triangulata-EXP2	Light-starved	Beads	3.8±0.2	n.d.	15.7±0.5	12.0
O. triangulata-EXP4a	Light-replete	FLBs	4.6±0.1	n.d.	25.1±0.1	20.5
O. triangulata-EXP4b	Light-replete	FLBs	7.2±0.8	n.d.	33.4±1.4	26.2

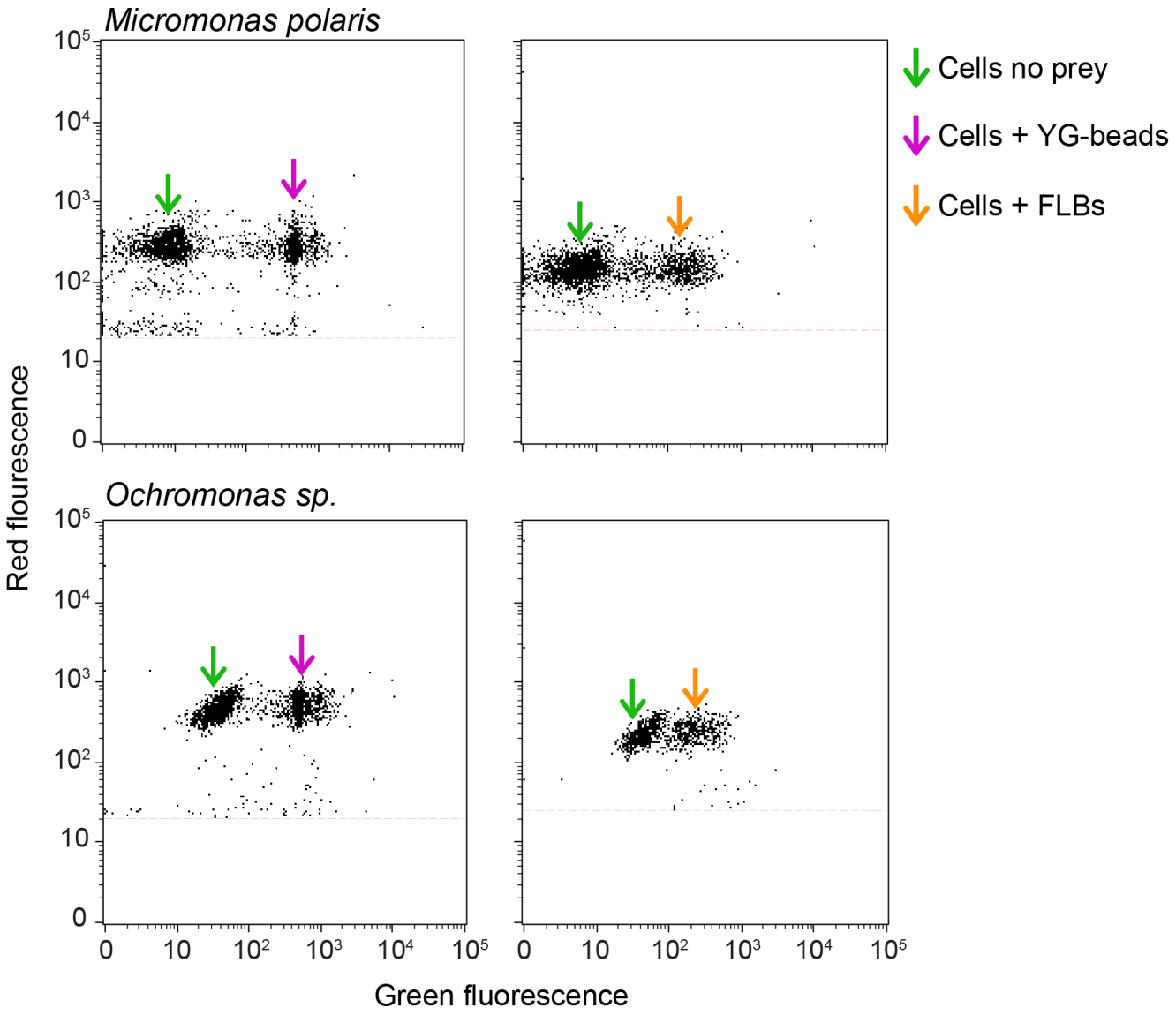

Figure S1. Flow cytometry cytograms.

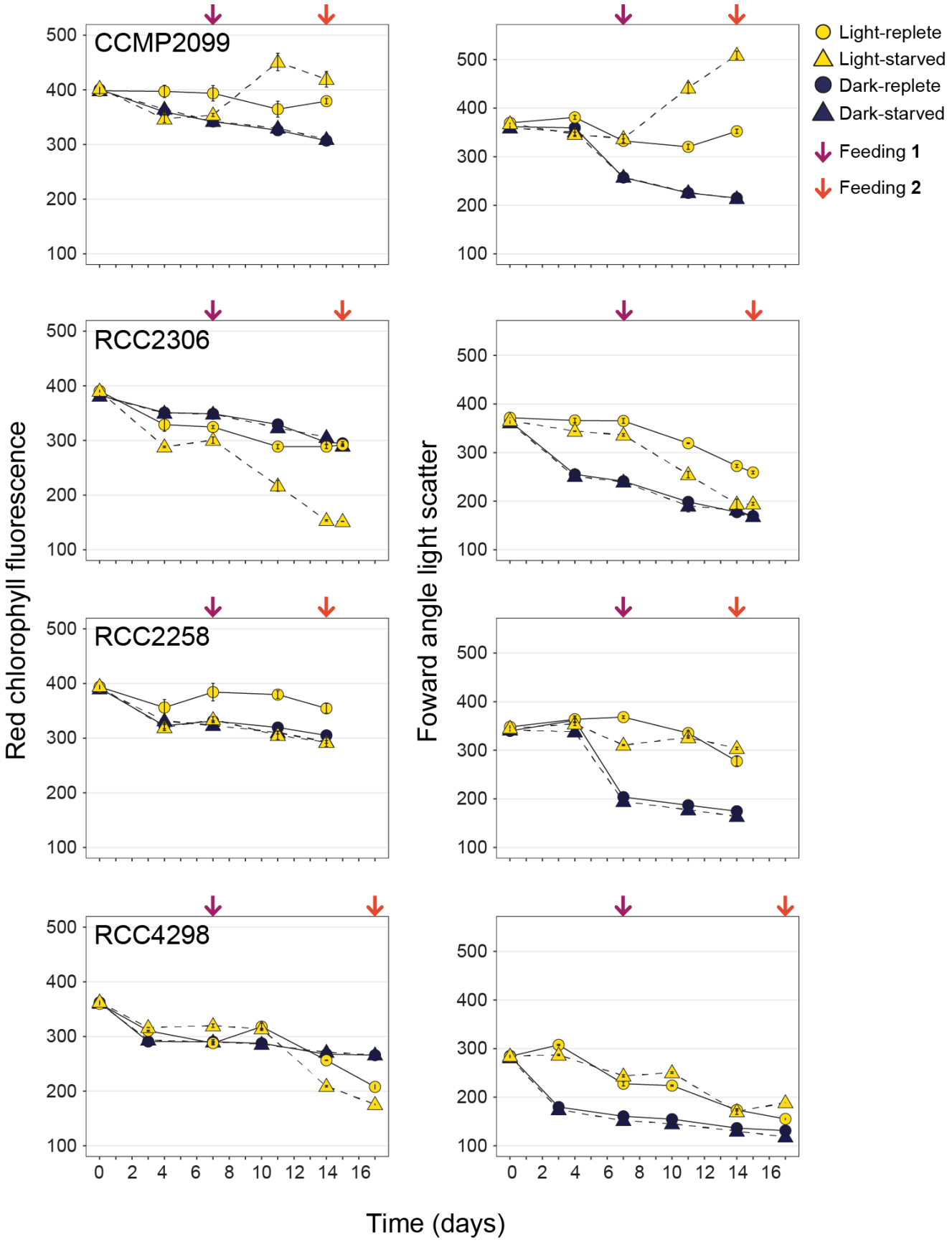

Figure S2. Change in forward scatter and red chlorophyll fluorescence measured by flow cytometry during the experiments reported in Figure 1 (*M. polaris*-EXP1).

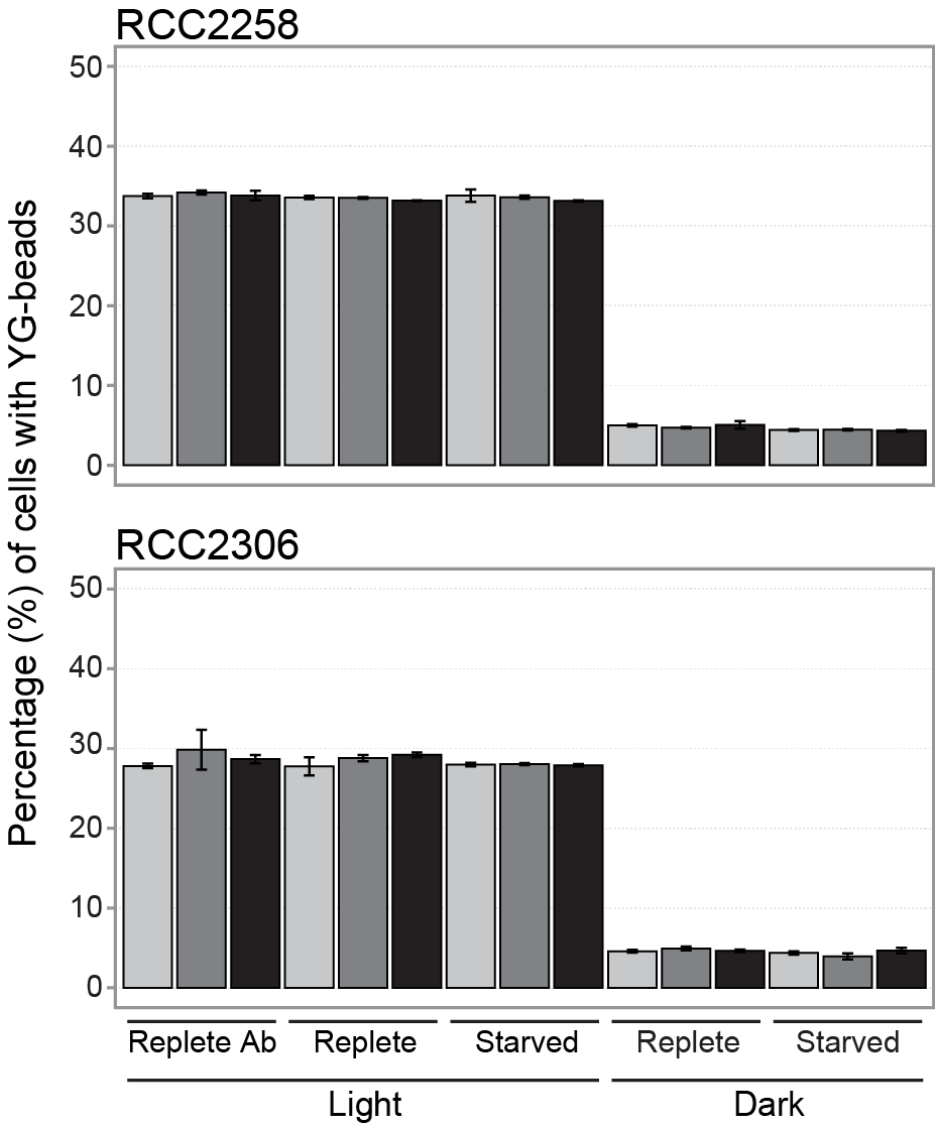

Figure S3. Percent of *M. polaris* cells with YG-beads (*M. polaris*-EXP2) for each strain and treatment. The first column correspond to feeding-1 and second column to feeding-2. The color of the bars represent the time point (in minutes) after the addition of YG-beads (0 minutes; light grey, 20 minutes; dark grey, 40 minutes; black).